Contents lists available at ScienceDirect

Heliyon

Corilagin ameliorates macrophages inflammation in atherosclerosis through TLR4-NFκB/MAPK pathway

Da Meng [a,1], Xin Deng [a,1], Yi Wu [b], Jingyi Wu [a], Yaqiong Zhang [a], JiaYu Zhang [c], Yi Zhao [a], Yanyun Che [a,*]

[a] Engineering Laboratory for National Healthcare Theories and Products of Yunnan Province, Yunnan University of Chinese Medicine, No. 1076 Yuhua Road, Chenggong District, Kunming 650500, Yunnan, China
[b] Institute of Traditional Chinese Veterinary Medicine, College of Veterinary Medicine, Nanjing Agricultural University, Nanjing, 210095, China
[c] School of Pharmacy, Binzhou Medical University, Yantai, Shandong, 264003, China

ABSTRACT

Corilagin, a polyphenolic tannic acid compound, showed significant anti-inflammatory activity in atherosclerotic mice. The present study aimed to evaluate the effect and mechanism of corilagin in atherosclerosis by *in vivo*, *in vitro* and in molecular docking strategies analysis. An atherosclerotic model was established by feeding ApoE$^{-/-}$ mice a high-fat diet. Murine RAW264.7 macrophages were cultured and induced with lipopolysaccharide (LPS). Treatment with corilagin had a marked inhibitory effect on the plaque area and lipid accumulation in atherosclerotic mice. Corilagin decreased the expression of iNOS and promoted the expression of CD206 in aortic plaque, as well as inhibited the production of proinflammatory factors in HFD-fed ApoE$^{-/-}$ mice and LPS-induced RAW264.6 cell. Corilagin also obviously inhibited the expression of TLR4, reduced the phosphorylation of the JNK, the protein expressions of p38 and NF-κB pathway. In addition, corilagin markedly diminished the nuclear translocation of NF-κBp65. Similarly, molecular docking study suggested that hydrogen bonds were detected between the corilagin and the five proteins (TLR4, Myd88, p65, P38, and JNK) with a significant "CDOCKER energy". These results showed that the antiatherosclerotic effect of corilagin against M1 macrophage polarization and inflammation via suppression the activation of TLR4-NFκB/MAPK signaling pathway. Therefore, corilagin could be a promising lead compound to develop drugs for the treatment of atherosclerosis.

1. Introduction

Atherosclerosis, a chronic cardiovascular disease, is one of the most common causes of mortality death in the elderly [1]. The pathogenesis of atherosclerosis was correlated with lipoprotein deposition, inflammatory response, plaque formation and calcification [2]. Inflammation acts as a common basis for the physiological and pathological changes throughout atherosclerosis initiation and development [3,4]. Atherosclerosis also is usually considered as a chronic inflammatory disease. Accumulating evidence demonstrates that macrophages play an important role in the resolution of inflammation [5,6]. Macrophages can polarize to generate two

---

Abbreviations

AS	Atherosclerosis
CD36	Scavenger receptor CD36
Cor	Corilagin
Dex	Dexamethasone
ERK	Extracellular regulated protein kinases
IL-18	Interleukin-18
IL-1β	Interleukin-1β
IL-6	Interleukin-6
iNOS	Inducible Nitric Oxide Synthase
IκBα	Inhibitors of NF-κB α
JNK	c-Jun N-terminal kinase
LOX-1	Lectin-like ox-LDL receptor-1
LPS	Lipopolysaccharide
MAPK p38	Mitogenactivated protein kinases p38
mTOR	Mammalian target of rapamycin
MyD88	Myeloiddifferentiationfactor88
NF-κB p65	Nuclear factor-κappaB p65
RT-PCR	Reverse Transcription-Polymerase Chain Reaction
SDS	Sodium dodecyl sulfate
SRA	Scavenger receptor A
TLR4	Toll-like receptor 4

subpopulations with different functions in response to inflammation, namely proinflammatory macrophages (M1) and immuno-modulatory alternatively activated macrophages (M2) [7]. An imbalance of macrophage M1/M2 polarization often causes inflammatory conditions. In addition, a large amount of proinflammatory cytokines, such as IL-6, IL-1β, IL-18 and TNF-α, are released by M1 macrophages after lipid uptake via multiple and complex mechanisms, which ultimately result in serious inflammation [8]. The inflammatory reaction in turn aggravates atherosclerotic plaque instability [9,10]. Therefore, modulation of macrophages inflammation has emerged as a crucial potential target for antiatherosclerosis therapy. Toll-like receptor 4 (TLR4) was the classic signaling pathway in macrophages inflammatory signaling cascades in atherosclerosis. Activation of TLR4 initiates the intracellular signaling pathways employing mitogen activated protein kinases (MAPKs) and transcriptional factor nuclear factor kappa B (NF-κB), which regulate the gene expression of pro-inflammatory cytokines and other inflammatory mediators. It was suggested that an absence of TLR4 or MyD88 could lead to reduction of formation of atherosclerotic plaques in mice [11]. Studies have shown that some active constituents separated form plant extracts such as Val-Glu-Gly-Tyr peptide from Genus *Ulva* and Flavonoids from *Sophora tonkinensis* could inhibit inflammatory reaction by regulating TLR4-NFκB/MAPK signaling pathway [12,13]. So inhibiting the activation of TLR4-NFκB/MAPK signaling pathway and alleviating the inflammatory reaction caused by macrophage polarization can provide ideas for anti-atherosclerosis research.

Corilagin is a polyphenolic tannic acid compound that is widely present in plants of the genus Hypophyllum. Clinical basic theoretical research showed that corilagin had antibacterial, antioxidant, anti-tumor, liver protection and anti-inflammatory activities [14–16]. Modern pharmacological research showed that corilagin could inhibit the development of atherosclerosis in piglets or rabbits by regulating the expression of matrix metalloproteinases (MMP)-1, -2 and -9 or inhibiting the proliferation of VSMC cells induced by ox-LDL [17,18]. In addition, researchers had also found that corilagin could reduce the release of pro-inflammatory cytokines by inhibiting TLR4 signaling pathway of monocytes/macrophages in *vitro* [19,20]. Macrophage polarization is closely related to TLR4 signaling pathway. However, the exact mechanism of polarization level of corilagin-regulated macrophages is not clear.

Molecular docking, a virtual computational tool, is used to predict the binding capacity and binding mode of receptor-drug molecular complexes, which is extensively in the screening potential lead compounds for new chemical entity. The crystal structure of TLR4, MyD88, NF-κB p65, MAPK p38, and MAPK JNK are reported and regarded to be effective targets of macrophage inflammation, which provides a basis for screening active ingredients against AS.

In the present study, the ApoE$^{-/-}$mice feeding with a high-fat diet, RAW264.7 cells induced with lipopolysaccharide (LPS) and molecular docking strategies analysis were applied to evaluate the effects and mechanisms of corilagin anti-inflammatory on atherosclerosis.

2. Materials and methods

2.1. Chemicals and antibodies

Corilagin (Cor, catalog no. E-0689, purity ≥ 98%) was purchased from Shanghai Tauto Biotech Co. Ltd. (China). Dexamethasone (Dex, Shanghai Qcbio Science & Technologies Co.), C-Jun N-terminal kinase (JNK, #26164-1-AP), p-JNK (#80024-1-RR),

extracellular regulated protein (ERK, #16443-1-AP), p-ERK (#28733-1-AP), mitogen-activ/ated protein kinases p38 (MAPK p38, #14064-1-AP), inducible Nitric Oxide Synthase (iNOS, #18985-1-AP), cyclooxygenase 2 (COX2, #66351-1-lg), nuclear factor-κappaB p65 (NF-κB p65, #66535-1g), Horseradish peroxidase (HRP) conjugated Affinipure Goat Anti-Mouse IgG (H+L) (#SA00001-1) and HRP conjugated Affinipure Goat Anti-Rabbit IgG (H+L) (#SA00001-2) were obtained from Proteintech Group, Inc. (Wuhan, China). p-p38 (#11581-1) was purchased from Signalway Antibody Co. Ltd. (USA). Inhibitors of NF-κBα (IκBα, #P25963) and p-IκBα (#P25963) were obtained from Cell Signaling Technology (Danvers, MA, USA). Antibody against β-actin (sc-47778) was purchased from Santa Cruz Biotechnology Inc. (Santa Cruz, CA, USA).

2.2. Animal experiments

The animal experiments were authorized by the Institutional Animal Care and Use Committee of Yunnan University of Chinese Medicine [SYxK(Yunnan)K2017-0005]. C57BL/6 WT mice and ApoE$^{-/-}$ mice on the C57BL/6 background (male, 6-8-week-old, body weight: 18 ± 2 g) were obtained from SPF (Beijing) Biotechnology Co. Ltd, China. Male mice were kept under standard laboratory conditions (temperature 22–25 °C and relative humidity 55–65%) with 12:12 dark/light. After one week of feeding acclimation, the C57BL/6 mice were fed with a standard chow diet and served as the normal control. Fourty male ApoE$^{-/-}$ mice were randomly divided into high-fat diet (HFD, containing 21% fat and 0.15% cholesterol), HFD plus the standard drug atorvastatin or corilagin groups. Atorvastatin was administered by oral gavage to the mice (10 mg/kg/day added to 0.5% Carboxymethyl cellulose solution). Corilagin was orally administered at the dose of 15, 30, and 60 mg/kg/day in a 0.5% Carboxymethyl cellulose solution (The dosage of oral administration in mice was carried out according to the literature [19,20]). Mice went through gavage once daily for 8 weeks.

2.3. Serum biochemical assays

Blood samples collected from the retroorbital plexus in mice were placed for 2 h at room temperature, followed by centrifugation at 3000 rpm for 15 min at 4 °C. Take the upper serum, and use it to detect four blood lipids and serum inflammatory factors. The concentration of total cholesterol (TC), triglycerides (TG), low-density lipoprotein cholesterol (LDL-C), high-density lipoprotein cholesterol (HDL-C) kits were analyzed by enzymatic colorimetric methods using commercial Kits from Nanjing Jiancheng Biological Engineering Research Institute (Nanjing, China). The cytokine levels of interleukin (IL)-6, interleukin (IL)-18, interleukin (IL)-1β and tumor necrosis factor (TNF)-α in ApoE$^{-/-}$ mice were detected by the corresponding specific enzyme-linked immunosorbent assay (ELISA) kits (Meiming, Jiangsu, China). These assays were performed in a blinded manner and in duplicates within each animal group.

2.4. Histological, morphometric analysis and immunofluorescence staining

Whole arteries, including the aortic arch, thoracic, and abdominal regions, were cut longitudinally, fixed, and then stained with Oil Red O for lipid measurement at the surface of the vascular wall. The aortic root was embedded in paraffin, and then the aortic root was cut into 5 μm slices from the aortic valve. Three consecutive slices were dewaxed with xylene, then hydrated with alcohol from low to high concentration, and the morphological analysis was carried out by hematoxylin-eosin and Movat five-color dyeing in references [21]. Moreover, Three consecutive slices were fixed, and fluorescent antibody nitric oxide synthase (iNOS) and mannose receptor 1 (CD206) diluted with a certain staining titer were dripped, and the staining analysis was carried out according to the literature to evaluate the polarization level of macrophages in aortic plaque [22]. In short, the sections were incubated with anti-inducible iNOS and CD206 antibody at 4 °C overnight, then incubated with an FITC conjugated goat anti-rabbit secondary antibody (1:200, Servicebio Biotechnology, Wuhan, China) or Cy3 conjugated goat anti-mouse secondary antibody (1:200, Servicebio Biotechnology, Wuhan, China) and mounted with DAPI (1:200, Boster Biological Technology, China). Images were obtained using a confocal microscope and were merged using Image Pro Plus.

2.5. Cell culture and treatment

According to the literature [23,24], RAW264.7 murine macrophages were supplied by the Kunming Cell Bank, Kunming Institute of Zoology, Chinese Academy of Sciences. The RAW264.7 cell was cultured in DMEM medium (Vivacell). The culture media were supplemented with 10% fetal bovine serum (FBS; Vivacell, 2225114) and $1 \times$ penicillin/streptomycin (Cytiva, J200044) at 37 °C in 5% CO$_2$. After pretreatment with corilagin (60, 120 and 240 μM) for 2 h, the cells were stimulated with 1 μg/mL LPS for 24 h.

2.6. Cell viability assay and measurement of inflammatory cytokines

The effect of Cor on cell viability was measured by MTT assay. Briefly, RAW264.7 cells (1×10^4 cells/well) were cultured in 96-well plates and exposed to Cor at indicated concentrations (0, 15, 30, 60, 120, 240, 480 μmol/mL) for 24 h. After incubation with 20 μL of MTT solution (5 mg/mL in PBS) for an additional 4 h at 37 °C, the supernatant solution was removed, 150 μL of DMSO was added to dissolve the formazan crystal, and the absorbance of each well was measured with a microtiter reader (Tecan Infinite 200, Switzerland) at a wavelength of 570 nm. The absorbance values for control cells were set as 1 for normalization.

The culture supernatant was collected, and the levels of pro-inflammatory cytokines, including NO, iNOS, IL-6, IL-1β and MCP-1 were detected using ELISA kit (Lianke Biotechnology, Shanghai, China) according to the manufacturer's instructions.
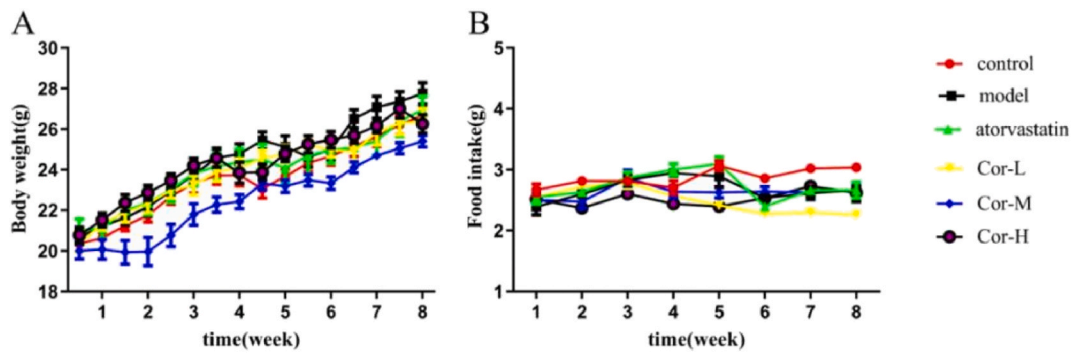
Fig. 1. Body weight and food intake of the ApoE$^{-/-}$ mice. (A) Bodyweight was determined once per week. (B) Food intake during the experiment. Data are mean $\pm$ SEM (n = 8).
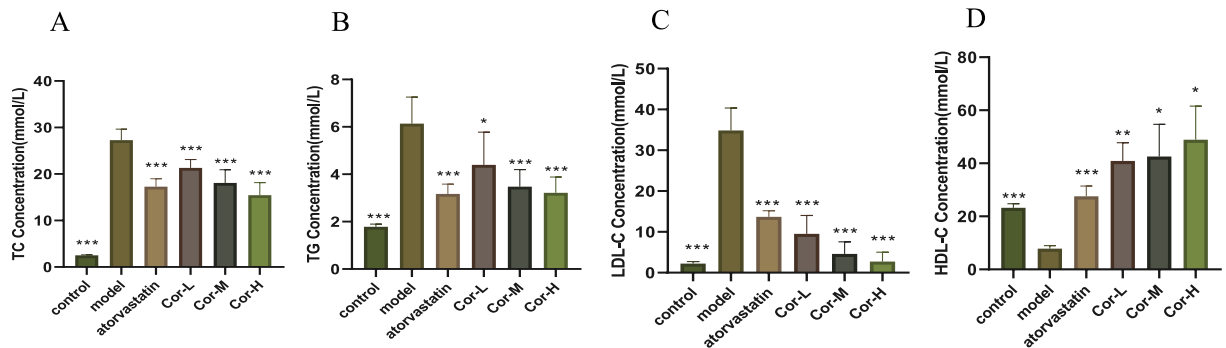
Fig. 2. Serum lipid profiles in the ApoE$^{-/-}$mice. (A) TC (B) TG (C) LDL-C (D) HDL-C. Data are mean $\pm$ SEM(n = 8). *$p < 0.05$, **$p < 0.01$, ***$p < 0.001$.
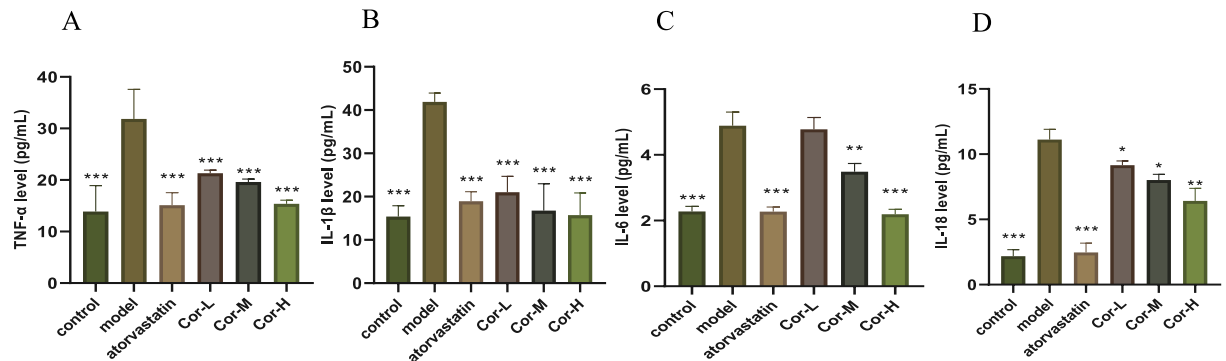
Fig. 3. The serum inflammatory cytokine levels in the ApoE$^{-/-}$ mice. (A) TNF-α (B) IL-1β (C) IL-6 (D) IL-18. Data are mean $\pm$ SEM (n = 8). *$p < 0.05$, **$p < 0.01$, ***$p < 0.001$.

2.7. Quantitative reverse transcription-polymerase chain reaction (qRT-PCR)

Total RNA was isolated from experimental cells using the miRNeasy kit according to the manufacturer's instructions, and was used as a template to synthesize cDNA for RT-qPCR. First strand cDNA was synthesized the using Thermo Scientific Maxima First Strand cDNA Synthesis kit. RT-qPCR was performed on a 7900HT real-time PCR system with the following cycling conditions: 1 PCR cycle, 95 °C, 10 min; 40 PCR cycles, 60 °C, 1 min, 95 °C, 15 s. RT-qPCR with SYBR Green dye was used to determine the expression of genes. Signals were analyzed by the ABI Prism Sequence Detection System. The 2$^{-\Delta\Delta Cq}$ method for relative quantification was used. β-Actin

A

B
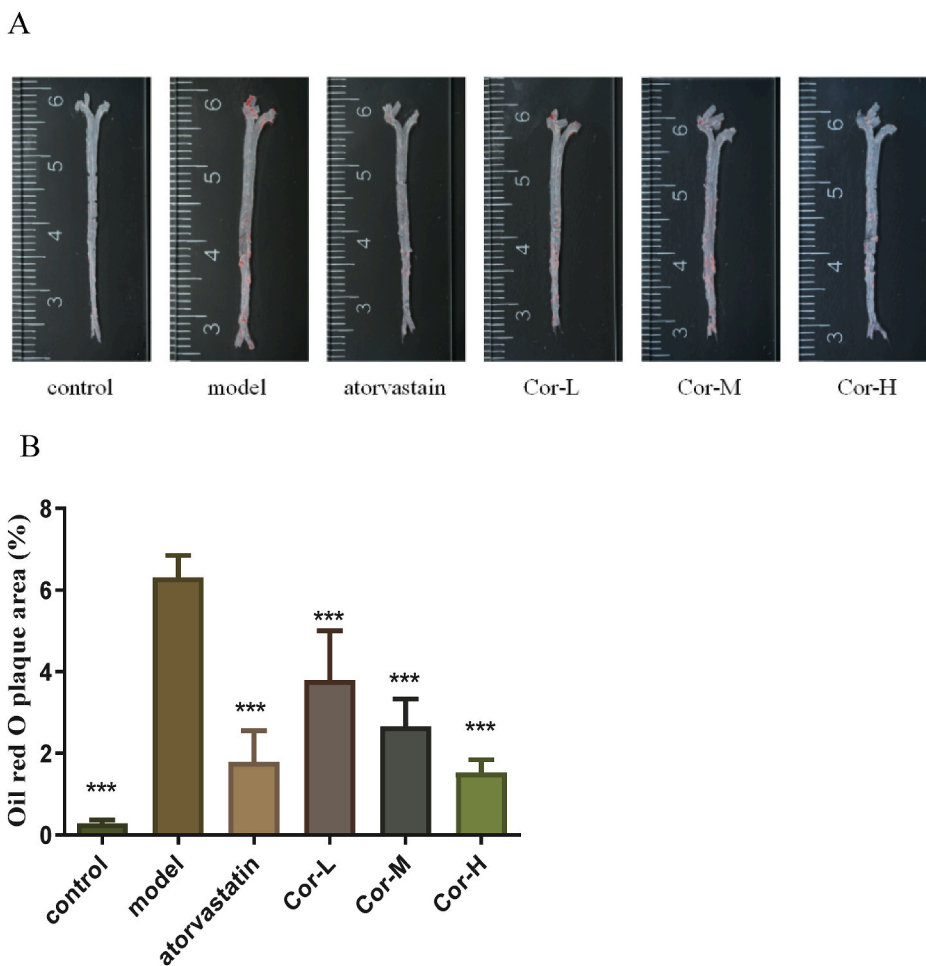
Fig. 4. The degree of AS in the aorta and aortic sinus in the ApoE$^{-/-}$ mice. (A) Representative photographs of aortic lumen stained by Oil red O. (B) Quantitative analysis of oil red O-positive areas of the aortic lumen relative to the total aortic area. (C) Cross-sections of the aortic sinus were stained by HE ($\times$100) (scale bars equal to 250 μm). (D) Cross-sections of the aortic sinus were stained by Movat ($\times$100) (scale bars equal to 250 μm). (E) Corresponding quantitative analysis on dye-positive areas. Data are mean $\pm$ SEM (n = 8). *$p < 0.05$, **$p < 0.01$, ***$p < 0.001$. (For interpretation of the references to color in this figure legend, the reader is referred to the Web version of this article.)

was used as an endogenous control. Each sample was run in triplicate. The following PCR primer sequences were used:

Gene	Forwarddir (5´-3´)	Reverse (5´-3´)
iNOS	CAAGCACATTTGGGAATGGAGA	CAGAACTGAGGGTACATGCTGGAG
IL-6	CCTTCACTCCATTCGCTGTCT	TCCTGATTTCCCTCATACTCG
IL-1β	FGGCAACCGTACCTGAACCCA	CCACGATGACCGACACCACC
MCP-1	TTAAAAACCTGGATCGGAACCAA	GCATTAGCTTCAGATTTACGGGT
TLR4	AGGGTTTCCTGTCAGTATCAAGTTT	TGATGCCTCCCTGGCTCCT
MyD88	TATACCAACCCTTGCACCAAGTC	CAGGCTCCAAGTCAGCTCATC
IκBα	GCCCTTCTGGGATTTCCT	GCGGCTCCGCTTCGTTCT
NF-κBp65	AGAGCAACCGAAACAGAGAGG	TTTGCAGGCCCCACATAGTT
β-actin	GTGACGTTGACATCCGTAAAGA	GTAACAGTCCGCCTAGAAGCAC

2.8. Western blotting analysis

Protein extracted from RAW264.7 cells was prepared with NP40 protein lysis buffer according to the manufacturer's instructions. The total protein concentrations in the extracts were determined with the BCA protein assay. Proteins were separated via SDS-PAGE (12%), electrotransferred onto polyvinylidene fluoride (PVDF) membranes, blocked with blocking buffer containing 5% (w/v) skimmed milk, and incubated in PBST (PBS with 0.1% w/v Tween-20) containing primary antibodies at 4 °C overnight. PVDF

C
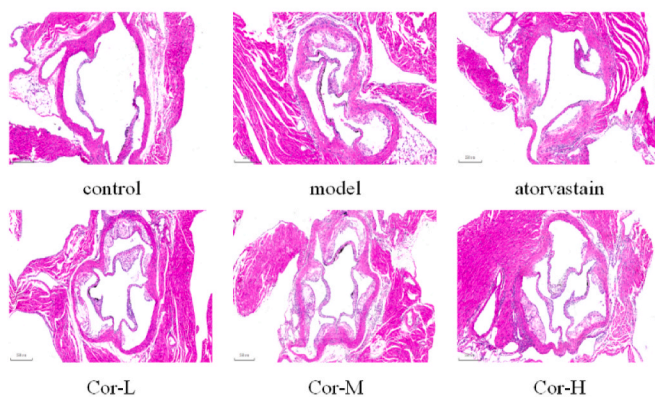
D
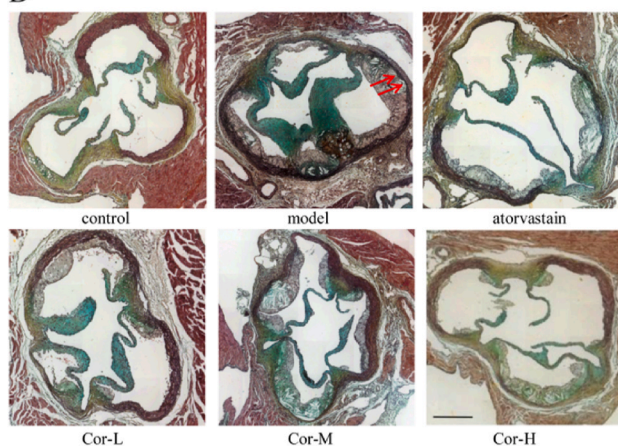
E
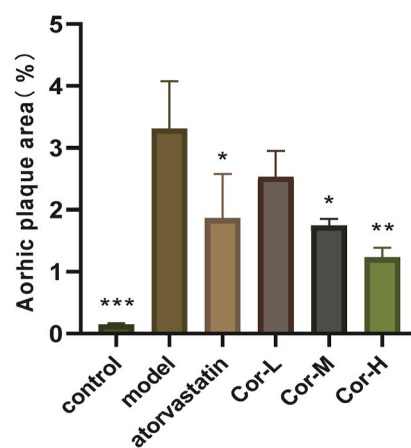
Fig. 4. (*continued*).

membranes were washed three times with PBST for 10 min each time and incubated with horseradish peroxidase for 1 h. Membranes were subsequently washed in the same way, and the hypersensitive ECL chemiluminescence kit was used for development after aspiration of liquid. Protein bands were quantified based on the mean ratio of the normalized integral optical density of β-actin or the protein.

2.9. Immunofluorescence staining in vitro

RAW264.7 cells were seeded at a density of 5×10^4 cells/mL on 6-well chamber slides. After incubation for 24 h, the medium was exchanged for medium containing Cor followed by another 1 h of incubation. Cells were then treated with LPS and incubated for 5 min. After incubation, cells were fixed with 4% formaldehyde, permeabilized with ice-cold MeOH, and treated with specific anti-p65 primary antibody overnight at 4 °C. After washing, goat anti-rabbit IgG H&L conjugated to Alexa Fluor 488-conjugated labeled secondary antibodies (Abcam) was used for visualization. For nuclear staining, cells were stained with Vectashield (Vector Laboratories, USA). The prepared cells were then observed under a confocal microscope (LSM700, Carl Zeiss, Germany), and images were recorded.

2.10. Molecular docking of Cor

Molecular docking experiment was performed by the AutoDock vina. Moreover, views of docking results were also completed through Discovery Studio 4.5 and PyMOL. When dealing with docking studies, the X-ray crystallographic structures of TLR4, MyD88, NF-κB p65, MAPK p38, and MAPK JNK from the Protein Data Bank (PDB, http://www.rcsb.org) were taken as the protein structures. The structure of Cor (compound CID: 73568) and Dex (compound CID: 5743) was downloaded from the PubChem website (https://pubchem.ncbi.nlm.nih.gov).
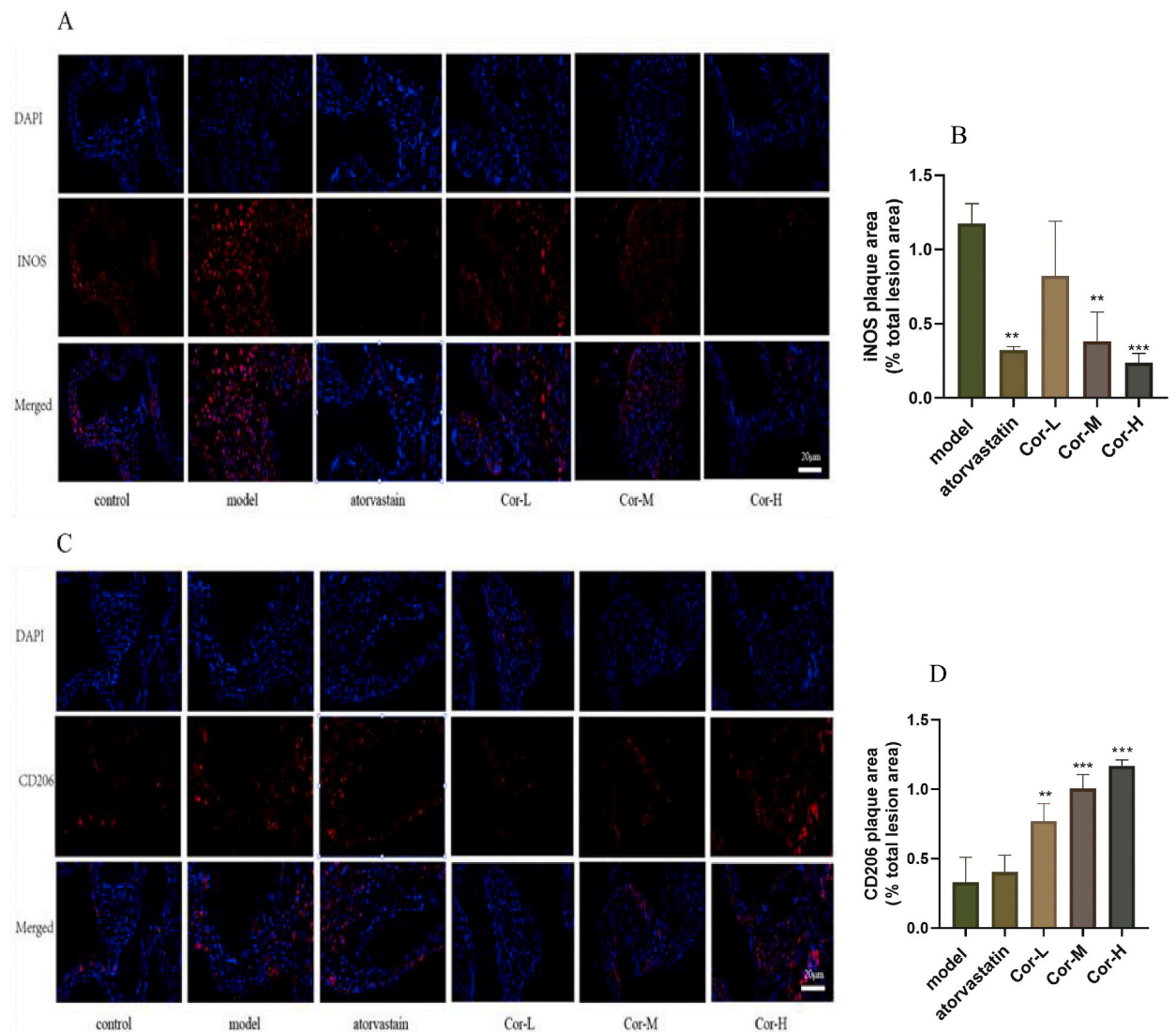
Fig. 5. Effects of Cor on macrophage polarization in atherosclerotic ApoE$^{-/-}$ mice. (A, B) immunofluorescence staining of the aortic root M1 marker iNOS (red), and a bar graph summarizing the results (n = 3, respectively). (C, D) immunofluorescence staining for M2 marker CD206 (red), and a bar graph summarizing the results (n = 3, respectively). Scale bar: 20 μm. Data are mean ± SEM. *$p < 0.05$, **$p < 0.01$, ***$p < 0.001$. (For interpretation of the references to color in this figure legend, the reader is referred to the Web version of this article.)

2.11. Statistical analysis

All data in this report are presented as mean ± standard derivation. One-way analysis of variance was performed for data analysis. The independent *t*-test that decided the statistical significance of differences among various groups as indicated by P < 0.05 (two-tailed) was performed with SPSS 26.0 (SPSS, Inc, Chicago, IL, USA).

3. Results

3.1. Body weight and food intake of ApoE$^{-/-}$ mice fed a high-fat diet

As shown in Fig. 1A and B, body weight gradually increased in the HFD-fed ApoE$^{-/-}$ mice compared with those of the normal diet-fed C57 mice, but there was no obvious difference. Similarly, food intake in Cor administered group compared to the control group was also no significant difference.
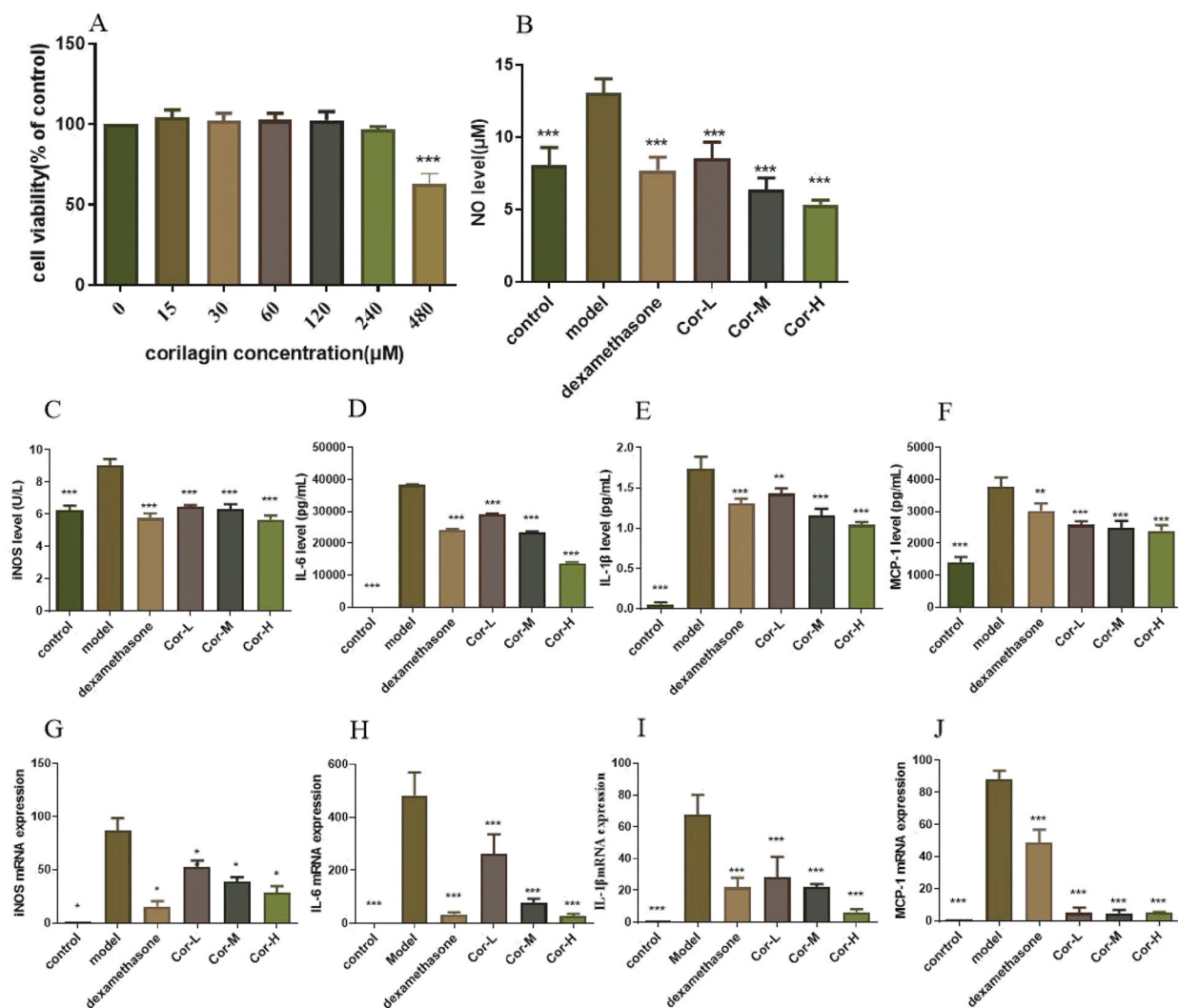
Fig. 6. Effects of Cor exposure on the macrophage survival and inflammatory cytokines. (A) Cell reproductive inhibition (B) NO (C) INOS (D) IL-6 (E) IL-1β (F) MCP-1 (G) iNOS mRNA expression (H) IL-6 mRNA expression (I) IL-1β mRNA expression (J) MCP-1 mRNA expression. Data are mean ± SEM (n = 3). *$p < 0.05$, **$p < 0.01$, ***$p < 0.001$.

3.2. The serum lipid profiles in the ApoE$^{-/-}$ mice

To confirm the hypolipidemic effect of Cor, serum lipid profiles were determined. ApoE$^{-/-}$ mice fed with a high fat-diet had greatly increased serum levels of TC, LDL-C, and TG and reduced levels of HDL-C compared with control animals (Fig. 2). The TC, TG, and LDL-C levels were significantly lower, while the HDL-C levels were efficiently higher in the atorvastatin and Cor than those in the model group.

3.3. Serum inflammatory cytokine levels in the ApoE$^{-/-}$ mice

To test the anti-inflammatory effect of Cor in HFD-induced ApoE$^{-/-}$ mice, we measured inflammatory mediators using ELISA. The levels of TNF-α, IL-1β, IL-6, and IL-18 in serum were significantly higher in the model group than those in the normal control group. As expected, the levels of these cytokines were inhibited by Cor and atorvastatin. The high-dose Cor showed a stronger effect than the low-dose Cor on the levels of all the cytokines except TNF-α and IL-1β (Fig. 3).

3.4. Atherosclerosis in the aorta and aortic sinus of the ApoE$^{-/-}$ mice

To estimate the effect of Cor on atherogenesis, our group tested a range of indicators of atherosclerosis in ApoE$^{-/-}$ mice. Our data showed that the plaque area of the aortic root of the positive drug group was obviously reduced, and the middle and high dose groups
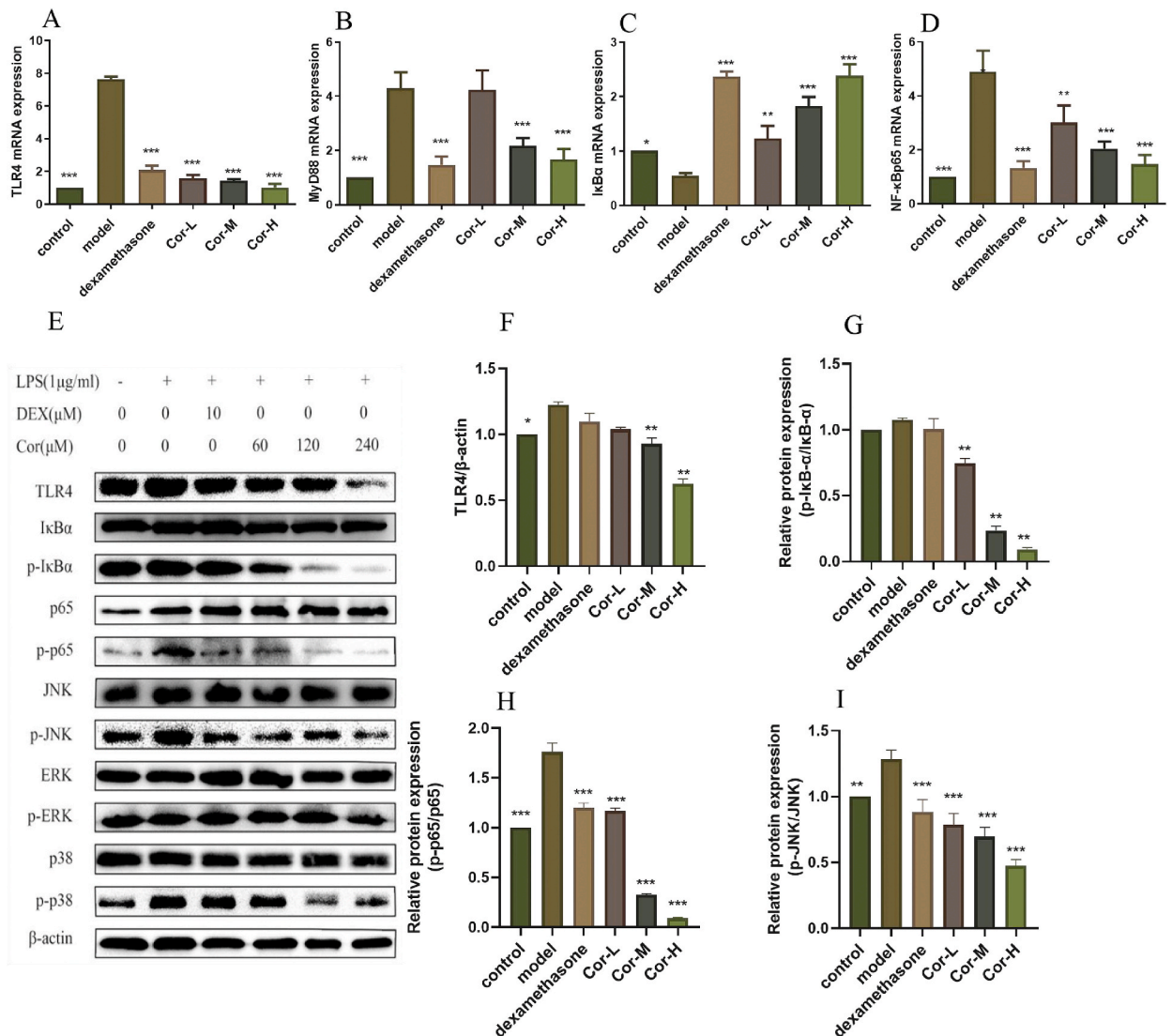
Fig. 7. Effect of Cor on the TLR4-dependent activation of NF-κB and MAPK by RAW264.7 stimulated by LPS. (A) TLR4 mRNA expression (B) MYD88 mRNA expression (C) IκBα mRNA expression (D) NF-κBp65 mRNA expression (E) total protein expression (F) TLR4 protein expression (G) p-IκB protein expression (H) p65 protein expression (I) JNK protein expression (J) p38 protein expression (K) ERK protein expression (L) p65 NF-κB nuclear translocation. Scale bars: 25 μm. Data are mean ± SEM (n = 3). *$p < 0.05$, **$p < 0.01$, ***$p < 0.00$.

of Cor significantly reduced the aortic plaque area of mice, compared to that of the model group in en face ORO-staining (Fig. 4A and B). Similar results were obtained from the H&E-stained frozen sections of the arterial sinus and ORO-stained frozen sections of the arterial roots (Fig. 4C). Moreover, the degenerated and broken vascular structure was improved to different degrees in both the positive drug group and the Cor group as compared with the model group in Movat staining (Fig. 4D and E).

3.5. Macrophage polarization marker expression in aortic root of ApoE$^{-/-}$ Mice

To explore whether Cor promotes favorable M1/M2 polarization within the plaque, we applied immunofluorescence to label M1 (iNOS) and M2 (CD206) macrophages. AS shown in Fig. 5, the expression of M1 macrophages was lower in the control group, but more in the model group. On the contrary, after middle and high-dose treatment with atorvastatin and Cor, the number of M1 macrophages decreased significantly (Fig. 5A and B). The number of M2 macrophages was the smallest in both the control group and the atorvastatin group. After each dose of Cor treatment, the number of M2 macrophages increased significantly (Fig. 5C and D).

Fig. 7. (*continued*).

Fig. 8. The docking results of Cor and Dex binding to TLR4-NF-κB/MAPK signaling pathway-related targets. The 3D interaction plot and 2D interaction plot of (A) TLR4, (B) MAPK JNK, (C) MAPK p38, (D) MyD88, (E) NF-κB p65. Red or pink dash line illustrate hydrophobic interactions.
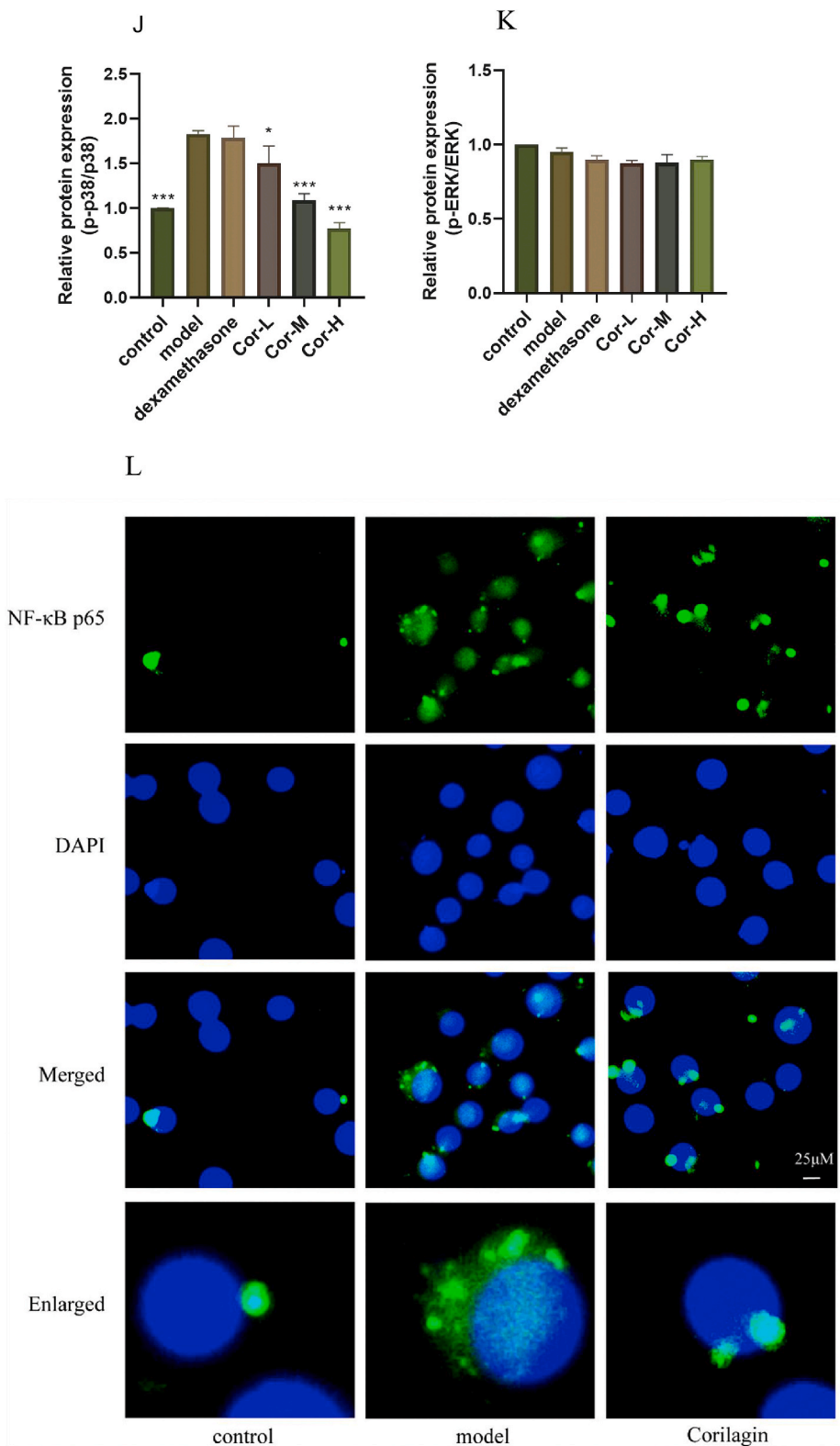
The green dash line indicates the hydrogen bond. (For interpretation of the references to color in this figure legend, the reader is referred to the Web version of this article.)

3.6. Effects of Cor exposure on the macrophage survival and inflammatory cytokines

The relative MTT values were not significantly different between the RAW264.7 macrophage cells receiving Cor at concentrations between 1 to 240 μM and the control. Therefore, concentrations of 60, 120, and 240 μM were selected for subsequent experiments (Fig. 6A).

ELISA assays were used to determine the proinflammatory cytokines and Greiss' reaction was used to estimate the NO generation. Upon stimulation with LPS (1 μg/mL), NO production, IL-6, IL-1β, and MCP-1 were markedly increased. However, treatment with Cor for 24 h could significantly reduce the production of NO, iNOS, IL-6, IL-1β, and MCP-1 compared with those in the ApoE$^{-/-}$ group (Fig. 6B–F). Furthermore, RT-PCR analysis was also conducted to determine the levels of these four indicators of Mrna expression in aortic arch tissue from the different group (Fig. 6G–J). As expected, Cor effectively suppressed the production of these indicators in RAW264.7 cell stimulated by LPS.

3.7. Cor inhibits the TLR4 and its downstream targets in RAW264.7 cells

Firstly, to investigate whether TLR4-NFκB signaling could be regulated by Cor, some key mRNA and proteins were detected. RT-PCR results demonstrated a significant concentration-dependent decrease in LPS-induced upregulation of TLR4, MYD88, and NFκB mRNA levels in Cor-treated RAW264.7 cells. In parallel, Cor was significantly associated with the increased IκBα mRNA expression in RAW264.7 cells in a dose-dependent manner (Fig. 7A–D). Western blot analysis showed that LPS increased the TLR4 in the RAW264.7 cells. However, the expression of TLR4 protein can be reduced to different degrees in groups with different doses of Cor. Meanwhile the phosphorylation of NF-κB/p65 and IκBα levels were significantly enhanced by LPS stimulation compared to the control group, and markedly down-regulated after Cor treatment compared to that of LPS-stimulated group (Fig. 7E–H). Similarly, Cor downregulated MAPK pathway in LPS-pre-treated cells as indicated by the significant reduction in p-p38 and p-JNK expression (Fig. 7E and I–K). In further studies, we found that LPS stimulation resulted in increased p65 translocation to the nucleus over the control group, and Cor treatment appeared to suppress this LPS-induced p65 translocation from the cytosol (Fig. 7L). Overall, these results suggested the substantial inhibition of Cor on TLR4 and its downstream.

3.8. Molecular dockings

We simulated Cor and Dex binding toTLR4, MAPK JNK, MAPK p38, MyD88 complex co-receptor within the Discovery Studio and PyMOL protein–ligand docking model. Cor had hydrogen bond interactions with TLR4, including residues Gly70, Tyr46 and Gly94 tight binding with TLR4. Simulation results indicated that the best binding affinity of Cor was −7.3 kcal/mol, and of Dexa, it was −7.0 kcal/mol, respectively (Fig. 8A). The benzene ring of Cor was found to hydrophobic interactions with residues of Val22, and it has hydrogen bond in Asp23, Tyr35 and Val22 to bind to MAPK JNK. Theoretical analysis and computer simulation results showed that the best binding affinities of Cor was −7.0 kcal/mol, and of Dex, it was −6.1 kcal/mol, respectively (Fig. 8B). Cor had hydrogen bond interactions with MAPK p38, including residues Gly110, Asp112, Asp168 and Asn155, also had hydrophobic interaction with residues Leu167, Ala51and Val38. The results demonstrated that the best binding affinity of Cor was −8.6 kcal/mol, and of Dex, it was −7.2 kcal/mol, respectively (Fig. 8C). Cor also had hydrogen bond interaction with MyD88 residues Gln181, Thr287, Phe285 and Trp286. It showed separately that the best binding affinity of Cor was −7.1 kcal/mol, of Dex, it was−6.8 kcal/mol (Fig. 8D). Cor had hydrogen bond interaction with NF-κB p65 residues His405 and Val469, also had hydrophobic interaction with residues Gln496 and Ala497. The results demonstrated that the best binding affinity of Cor was −7.9 kcal/mol, and of Dex, it was −7.2 kcal/mol, respectively 05 and Val469 through hydrogen bond interaction. (Fig. 8E). In conclusion, these data proved that Cor has a good binding effect with TLR4-MAPK/NF-κB signaling pathway-related proteins, which may be targeted for Cor to exert anti-inflammatory effects in AS.

4. Discussion

In the present research, the important findings were the anti-atherosclerotic effect of Cor against M1 macrophage polarization and inflammation via suppression the activation of TLR4-MAPK/NF-κB signaling pathway *in vivo* and *in vitro*. First of all, we observed the protective effect of Cor against the development of atherosclerosis. Treatment with Cor had a significant inhibitive effect on the plaque area and the lipid accumulation in the aortic sinus of atherosclerotic mice. Inflammation are major contributors to foam cell formation during the development of atherosclerosis. Macrophage polarization plays a crucial role in Inflammation [25]. A large amount of proinflammatory cytokines, such as IL-6, IL-1β, IL-18 and TNF-α, are released by M1 macrophages after lipid uptake via multiple and complex mechanisms, which ultimately result in serious inflammation [26]. In this study, the experimental results showed that Cor inhibited the production of TNF-α, IL-1β, IL-6, IL-18 in HFD-fed ApoE$^{-/-}$ mice and LPS-induced RAW264.6 cell. Next, we found that Cor decreased the expression of iNOS and promoted the expression of CD206 in aortic plaque. M1 macrophages are known to have pro-inflammatory effects, and iNOS are markers of the M1 phenotype. The M2 phenotype has anti-inflammatory effects and is characterized by the specific expression of CD206. Animal experiments demonstrated that Cor skew the M1-like phenotype to the M2-like phenotype and inhibit the inflammatory response. Furthermore, we used LPS-stimulated macrophages to study the activation and induction of macrophage M1-like polarization. The results showed that the M1 markers and pro-inflammatory factors significantly
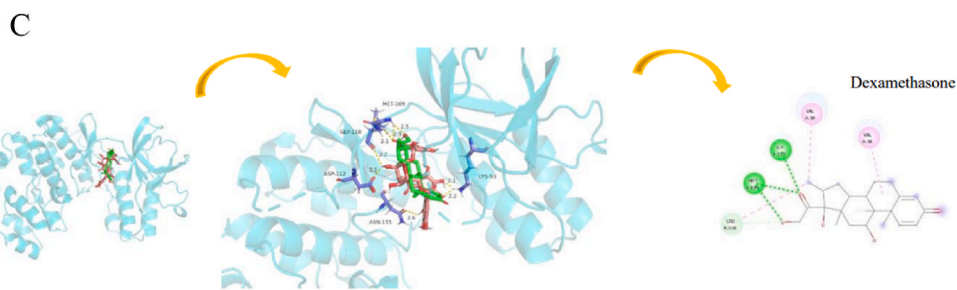
Fig. 8. (*continued*).

E
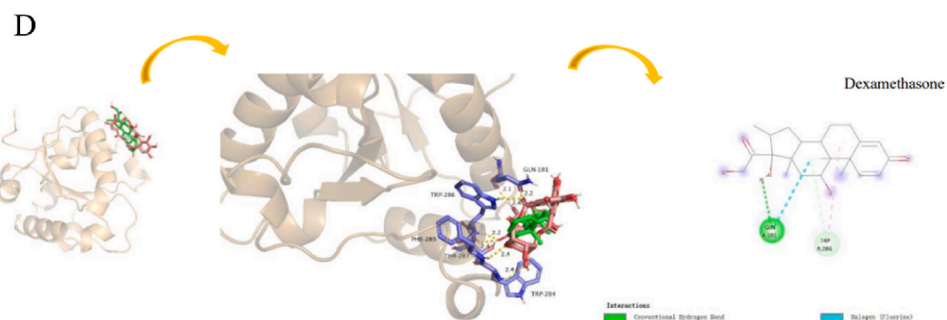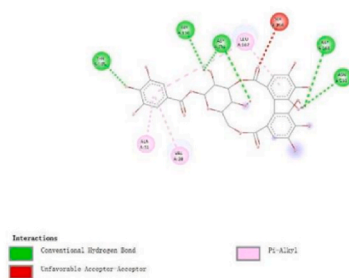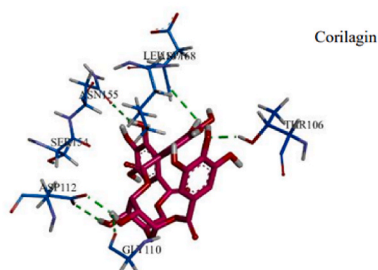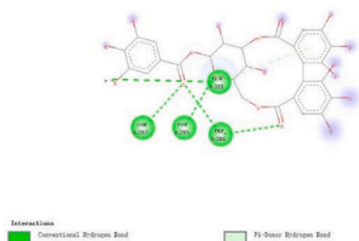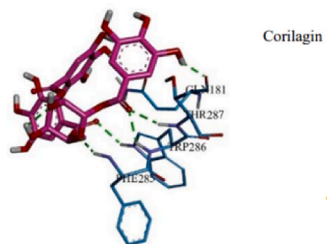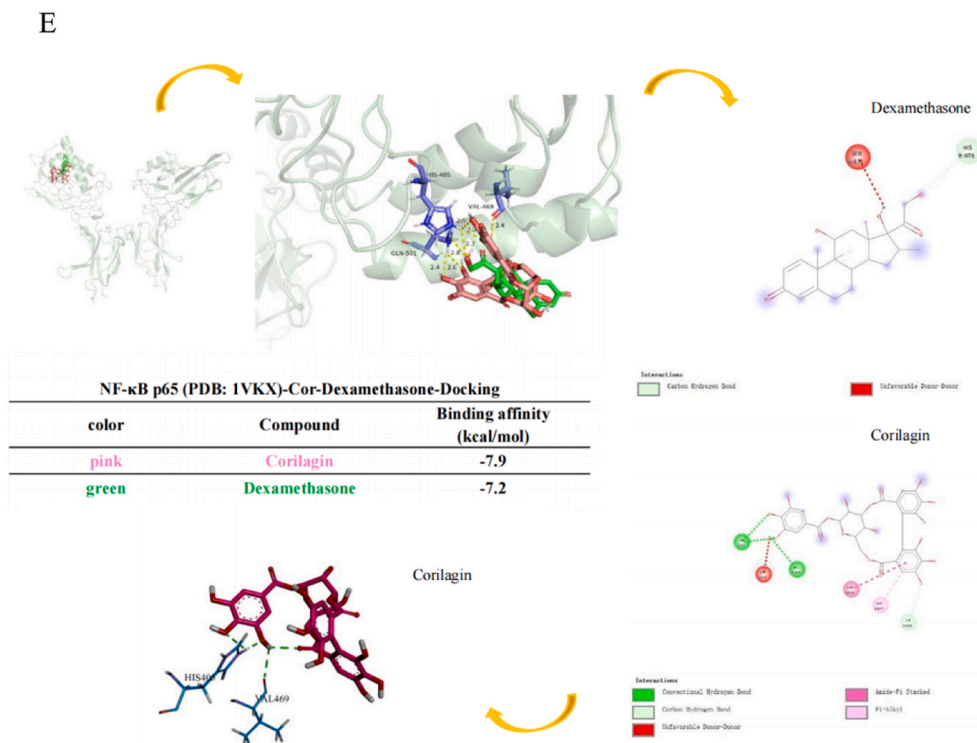
Fig. 8. (*continued*).

increased after LPS stimulation. These results indicated that Cor could regulate the polarization of macrophages. However, this study did not detect the effect of Cor on the phenotype of macrophages, and Flow cytometry (FCM) will be used for further research in the future.

The phenotypic changes and functions of macrophages are regulated by various signaling pathways. Transcription factors, including TLR4-NF-κB and TLR4-MAPK, are involved in M1 programming [8]. TLR4-NF-κB pathway has widely been considered as a classical pro-inflammatory signaling pathway [27]. When exposed to stimulus such as LPS, p65/p50 heterodimer (IκBα) are phosphorylated and degraded by activation of IKKs, which result in p65/p50 nuclear translocation. Eventually, the transcription of NF-κB target genes is activated [28]. To explore if the NF-κB pathway is involved in reversing the action of Cor for LPS-stimulated M1 polarization. Our results verified that the presence of Cor suppressed activation of NF-κB induced by LPS, decreased phosphorylation of IκBα, and reduced nuclear translocation of NF-κB p65 and its phosphorylation. In addition, given that the TLR4-MAPK pathway is also a critical pro-inflammatory signaling pathway and especially JNK and p38 are widely considered motivators of IκBα degradation [29–31], we also examined whether the anti-M1 polarization mechanism of Cor associated with the MAPK pathway. Cor significantly inhibited the phosphorylation levels of JNK and p38 as we expected. These results suggested that TLR4-NF-κB and TLR4-MAPK/JNK/p38 pathways were involved in improvement of Cor for LPS-promoted M1 polarization.

A growing number of molecular docking experiments have been applied in the research of the binding sites or targets of natural compounds [31–33]. In this study, based on the molecular docking experiments, it was found that Cor could form stable binding to several key nodes (TLR4, MyD88, NF-κBp65, MAPK P38, and MAPK JNK) in macrophage inflammation, among which MAPK P38 is supposed to embrace the highest interaction energy. To sum up, Cor may act on the TLR4-NF-κB/MAPK pathway with a multi-target effect, which in agreement with the corresponding experimental results of cells.

Modern pharmacological research shows that inflammation is closely related to atherosclerosis, and TLR4-NF-κB/MAPK pathway is one of the classic pathways to regulate inflammation, and Cor can significantly inhibit inflammation. Some scholars have found that corilagin can regulate the expression of TLR4 protein, but it is not clear whether it can inhibit the polarization of macrophage M1 by regulating TLR4-NF-κB/MAPK pathway, so this paper studies it. However, in this paper the macrophage-associated inflammatory effects and pathways of Cor only be discussed, the specific target protein of Cor need to be studied further with the methods of Surface Plasmon Resonance (SPR), or with the validated experiment in model of knockout of target gene in mice in order to provide a basis for clinical application and resource development and utilization.

5. Conclusion

In this work, we identified Cor as an effective compound to treat AS. Importantly, we demonstrate a new mechanism of the regulation of macrophage polarization of Cor on AS, by which Cor inhibits macrophage inflammation and prevents the development of

AS.

Author contributions

1 Yanyun Che and Yi Zhao conceived and designed the experiments;
2 Da Meng, Xin Deng and Yi Wu performed the experiments;
3 Jingyi Wu and Yaqiong Zhang analyzed and interpreted the data;
4 Yaqiong Zhang and JiaYu Zhang contributed reagents, materials, analysis tools or data;
5 Da Meng wrote the paper.

All of the authors have read and approved the final submitted manuscript.

Data availability statement

The data that support the findings of this study are available from the corresponding author upon reasonable request.

Declaration of competing interest

The authors declare that they have no known competing financial interests or personal relationships that could have appeared to influence the work reported in this paper

Acknowledgments

Appendix A. Supplementary data

Supplementary data to this article can be found online at https://doi.org/10.1016/j.heliyon.2023.e16960.

References

[1] L. Peter, E.B. Julie, B. Lina, et al., Atherosclerosis, Nat. Rev. Dis. Prim. 5 (1) (2019) 56, https://doi.org/10.1038/s41572-019-0106-z.
[2] F. Schaftenaar, V. Frodermann, J. Kuiper, et al., Atherosclerosis: the interplay between lipids and immune cells, Curr. Opin. Lipidol. 27 (3) (2016) 209–215, https://doi.org/10.1097/MOL.0000000000000302.
[3] Y. Zhu, X. Xian, Z. Wang, et al., Research progress on the relationship between atherosclerosis and inflammation, Biomolecules 8 (3) (2018) 80, https://doi.org/10.3390/biom8030080.
[4] G.R. Geovanini, P. Libby, Atherosclerosis and inflammation: overview and updates, Clin. Sci. (Lond.) 132 (12) (2018) 1243–1252, https://doi.org/10.1042/CS20180306.
[5] K. Hamidzadeh, S.M. Christensen, E. Dalby, et al., Mosser. Macrophages and the recovery from acute and chronic inflammation, Annu. Rev. Physiol. 79 (2017) 567–592, https://doi.org/10.1146/annurev-physiol-022516-034348.
[6] S. Watanabe, M. Alexander, A.V. Misharin, et al., Budinger. The role of macrophages in the resolution of inflammation, J. Clin. Invest. 129 (7) (2019) 2619–2628, https://doi.org/10.1172/JCI124615.
[7] P. Libby, Inflammation in atherosclerosis, Arterioscler. Thromb. Vasc. Biol. 32 (9) (2012) 2045–2051, https://doi.org/10.1161/ATVBAHA.108.179705.
[8] X. Jian, Y. Liu, Z. Zhao, et al., The role of traditional Chinese medicine in the treatment of atherosclerosis through the regulation of macrophage activity, Biomed. Pharmacother. 118 (2019) 109375, https://doi.org/10.1016/j.biopha.2019.109375.
[9] S. Yang, H.Q. Yuan, Y.M. Hao, et al., Macrophage polarization in atherosclerosis, Clin. Chim. Acta 501 (2020) 142–146, https://doi.org/10.1016/j.cca.2019.10.034.
[10] A. Shapouri-Moghaddam, S. Mohammadian, H. Vazini, et al., Macrophage plasticity, polarization, and function in health and disease, J. Cell. Physiol. 233 (9) (2018) 6425–6440, https://doi.org/10.1002/jcp.26429.
[11] M.H. Roshan, A. Tambo, N.P. Pace, The role of TLR2, TLR4, and TLR9 in the pathogenesis of atherosclerosis, Int. J. Inflamm. (2016), 1532832, https://doi.org/10.1155/2016/1532832.
[12] W. Xia, P. Luo, P. Hua, et al., Discovery of a new Pterocarpan-type antineuroinflammatory compound from Sophora tonkinensis through suppression of the TLR4/NFκB/MAPK signaling pathway with PU.1 as a potential target, ACS Chem. Neurosci. 10 (1) (2019) 295–303, https://doi.org/10.1021/acschemneuro.8b00243.
[13] R.E. Cian, C. Hernández-Chirlaque, R. Gámez-Belmonte, et al., Martínez-Augustin. Green Alga Ulva spp. hydrolysates and their peptide fractions regulate cytokine production in splenic macrophages and lymphocytes involving the TLR4-NFκB/MAPK pathways, Mar. Drugs 16 (7) (2018) 235, https://doi.org/10.3390/md16070235.
[14] X. Li, Y. Deng, Z. Zheng, et al., Corilagin, a promising medicinal herbal agent, Biomed. Pharmacother. 99 (2018) 43–50, https://doi.org/10.1016/j.biopha.2018.01.030.
[15] W. Widowati, H.S.W. Kusuma, S. Arumwardana, et al., Corilagin potential in inhibiting oxidative and inflammatory stress in LPS-induced murine macrophage cell lines (RAW 264.7), Iran J Basic Med Sci 24 (12) (2021) 1656–1665, https://doi.org/10.22038/IJBMS.2021.59348.13174.
[16] F.C. Liu, H.P. Yu, A.H. Chou, et al., Corilagin reduces acetaminophen-induced hepatotoxicity through MAPK and NF-κB signaling pathway in a mouse model, Am J Transl Res 12 (9) (2020) 5597–5607, eCollection 2020.

[17] B. He, D. Chen, X.C. Zhang, et al., Antiatherosclerotic effects of corilagin via suppression of the LOX-1/MyD88/NF-κB signaling pathway in vivo and in *vitro*, J. Nat. Med. 76 (2) (2022) 389–401, https://doi.org/10.1007/s11418-021-01594-y.

[18] Y.T. Tao, R.H. Yang, Y.Z. Yang, et al., Corilagin ameliorates atherosclerosis by regulating MMP-1, -2, and -9 expression in vitro and in vivo, Eur. J. Pharmacol. 906 (2021), 174200, https://doi.org/10.1016/j.ejphar.2021.174200.

[19] Y. Li, Y. Wang, Y. Chen, et al., Corilagin ameliorates atherosclerosis in Peripheral artery disease via the toll-like receptor-4 signaling pathway in vitro and in *vivo*, Front. Immunol. 11 (2020) 1611, https://doi.org/10.3389/fimmu.2020.01611. Published 2020 Aug 6.

[20] H. Lv, L. Hong, Y. Tian, et al., Corilagin alleviates acetaminophen-induced hepatotoxicity via enhancing the AMPK/GSK3β-Nrf2 signaling pathway, Cell Commun. Signal. 17 (1) (2019) 2, https://doi.org/10.1186/s12964-018-0314-2. Published 2019 Jan 10.

[21] S. Fang, S. Sun, H. Cai, et al., IRGM/Irgm1 facilitates macrophage apoptosis through ROS generation and MAPK signal transduction: Irgm1(+/-) mice display increases atherosclerotic plaque stability, Theranostics 11 (19) (2021) 9358–9375, https://doi.org/10.7150/thno.62797. Published 2021 Sep. 9.

[22] S. Franco, A. Stranz, F. Ljumani, et al., Role of FOXM1 in vascular smooth muscle cell survival and neointima formation following vascular injury, Heliyon 6 (6) (2020), e04028, https://doi.org/10.1016/j.heliyon.2020.e04028. Published 2020 Jun 16.

[23] K. Shirato, T. Kizaki, SARS-CoV-2 spike protein S1 subunit induces pro-inflammatory responses via toll-like receptor 4 signaling in murine and human macrophages, Heliyon 7 (2) (2021), e06187, https://doi.org/10.1016/j.heliyon.2021.e06187. Published 2021 Feb 2.

[24] S. Wei, T. Wang, Q. Cao, et al., Anti-inflammatory effects of Torin2 on lipopolysaccharide-treated RAW264.7 murine macrophages and potential mechanisms, Heliyon 8 (7) (2022), e09917, https://doi.org/10.1016/j.heliyon.2022.e09917. Published 2022 Jul 9.

[25] Z. Wang, X. Zhang, L. Zhu, et al., Inulin alleviates inflammation of alcoholic liver disease via SCFAs-inducing suppression of M1 and facilitation of M2 macrophages in mice, Int. Immunopharm. 78 (2020), 106062, https://doi.org/10.1016/j.intimp.2019.106062.

[26] M. Ban, H. Su, X. Zeng, et al., An active fraction from Spatholobus suberectus dunn inhibits the inflammatory response by regulating microglia activation, switching microglia polarization from M1 to M2 and suppressing the TLR4/MyD88/NF-κB pathway in LPS-stimulated BV2 cells, Heliyon 9 (4) (2023), e14979, https://doi.org/10.1016/j.heliyon.2023.e14979.

[27] A. Hoter, M.E. El-Sabban, H.Y. Naim, The HSP90 family: structure, regulation, function, and implications in health and disease, Int. J. Mol. Sci. 19 (9) (2018) 2560, https://doi.org/10.3390/ijms19092560.

[28] P. Viatour, M.P. Merville, V. Bours, et al., Phosphorylation of NF-kappaB and IkappaB proteins: implications in cancer and inflammation, Trends Biochem. Sci. 30 (1) (2005) 43–52, https://doi.org/10.1016/j.tibs.2004.11.009.

[29] S.I. Jang, H.J. Kim, Y.J. Kim, et al., Tanshinone IIA inhibits LPS-induced NF-kappaB activation in RAW 264.7 cells: possible involvement of the NIK-IKK, ERK1/2, p38 and JNK pathways, Eur. J. Pharmacol. 542 (1–3) (2006) 1–7, https://doi.org/10.1016/j.ejphar.2006.04.044.

[30] Y.H. Lee, W.P. Schiemann, Fibromodulin suppresses nuclear factor-kappaB activity by inducing the delayed degradation of IKBA via a JNK-dependent pathway coupled to fibroblast apoptosis, J. Biol. Chem. 286 (8) (2011) 6414–6422, https://doi.org/10.1074/jbc.M110.168682.

[31] Y.T. Yeung, F. Aziz, A. Guerrero-Castilla, et al., Signaling pathways in inflammation and anti-inflammatory therapies, Curr. Pharmaceut. Des. 24 (14) (2018) 1449–1484, https://doi.org/10.2174/1381612824666180327165604.

[32] M.A. Morsy, A.A.K. El-Sheikh, A.R.N. Ibrahim, et al., In silico and in vitro identification of secoisolariciresinol as a re-sensitizer of P-glycoprotein-dependent doxorubicin-resistance NCI/ADR-RES cancer cells, PeerJ 10 (2020), https://doi.org/10.7717/peerj.9163, 8:e9163. 8:e9163.

[33] D.L. Penkler, Tastan Bishop Ö. Modulation of human Hsp90α Conformational dynamics by allosteric ligand interaction at the C-terminal domain, Sci. Rep. 9 (1) (2019) 1600, https://doi.org/10.1038/s41598-018-35835-0.